Electrostatic analysis of n-doped $SrTiO_3$ metal-insulator-semiconductor systems

A. M. Kamerbeek,[1,a)] T. Banerjee,[1] and R. J. E. Hueting[2]
[1]*Physics of Nanodevices, Zernike Institute for Advanced Materials, University of Groningen, Nijenborgh 4, 9747 AG Groningen, The Netherlands*
[2]*Semiconductor Components, MESA+ Institute for Nanotechnology, University of Twente, 7500 AE Enschede, The Netherlands*

(Received 2 June 2015; accepted 19 November 2015; published online 11 December 2015)

Electron doped $SrTiO_3$, a complex-oxide semiconductor, possesses novel electronic properties due to its strong temperature and electric-field dependent permittivity. Due to the high permittivity, metal/n-$SrTiO_3$ systems show reasonably strong rectification even when $SrTiO_3$ is degenerately doped. Our experiments show that the insertion of a sub nanometer layer of AlO_x in between the metal and n-$SrTiO_3$ interface leads to a dramatic reduction of the Schottky barrier height (from around 0.90 V to 0.25 V). This reduces the interface resistivity by 4 orders of magnitude. The derived electrostatic analysis of the metal-insulator-semiconductor (n-$SrTiO_3$) system is consistent with this trend. When compared with a Si based MIS system, the change is much larger and mainly governed by the high permittivity of $SrTiO_3$. The non-linear permittivity of n-$SrTiO_3$ leads to unconventional properties such as a temperature dependent surface potential non-existent for semiconductors with linear permittivity such as Si. This allows tuning of the interfacial band alignment, and consequently the Schottky barrier height, in a much more drastic way than in conventional semiconductors. © *2015 AIP Publishing LLC*. [http://dx.doi.org/10.1063/1.4936959]

I. INTRODUCTION

There is a wide interest in devices which utilize an ultra-thin insulating layer between rectifying metal/semiconductor (MS) contacts, for instance, to reduce contact resistance in semiconducting devices or to allow spin injection in the semiconductor.[1–4] For $SrTiO_3$, there is additional interest, since metal/n-$SrTiO_3$ contacts often behave as a metal/insulator/semiconductor (MIS) due to the presence of an electronic dead layer.[5–7] Furthermore, a gated two-dimensional electron gas (2DEG) at oxide/$SrTiO_3$ interfaces, with $LaAlO_3$ or γ-Al_2O_3 oxides, comprises a MIS system.[8,9] Earlier it was reported that the dielectric permittivity of $SrTiO_3$ depends both on electric field (E) and on temperature (T).[10,11] This makes the analysis and modeling of the $SrTiO_3$-based M(I)S-system less straightforward compared with its linear dielectric counterparts such as Si.

Here, we derive an electrostatic model which describes the potential landscape at the interface as a function of gate action, temperature, and interfacial insulator thickness for the MI/n-$SrTiO_3$ system. The surface potential in an MI/n-$SrTiO_3$ system is shown to have a more complex dependence on the gate bias compared with conventional semiconductors with a constant permittivity. In an earlier work, a reduction of the Schottky Barrier Height (SBH) by the insertion of a thick polar insulator has been reported while still exhibiting high resistive rectifying contacts.[12] Recently, a large reduction of the contact resistance was achieved by inserting a sub-nanometer thick insulating layer where the reduction in SBH is ascribed to the polar nature of the insulator.[13] In this work, we realize low resistive, tunneling contacts, by the insertion of an ultra-thin non-polar insulator (AlO_x). This reduction is driven by the large value of $SrTiO_3$'s permittivity (ε_s). The analysis of the temperature dependent Current-Voltage (I-V) measurements of our Co/AlO_x/n-$SrTiO_3$ diodes verifies the strong SBH reduction. The reduction is much larger than for conventional semiconductors and occurs even in the absence of Fermi level pinning. The non-linear nature of ε_s also leads to other surprising features such as a temperature dependent SBH not present for metal/n-$SrTiO_3$ or conventional MIS systems. These results are important for understanding the electrostatics in gated oxide/$SrTiO_3$ 2DEGs and spin injection experiments in Nb-doped $SrTiO_3$ and for designing novel electronics using such an M/I/n(p)-$SrTiO_3$ structure.

II. ELECTROSTATIC MODEL

In our analysis, we assume the following in the M(I)S system: (1) there are only ideal interfaces: no gap states, traps, or fixed charge[14,15] and (2) the system is in low injection operation (low forward and reverse bias, thus ignoring hole charge). For convenience sake, we use $x = 0$ as the depletion edge and $x = W$ (W is the depletion width) refers to the M(I)S interface, see also Fig. 1.

First, we focus on the Schottky diode (or MS system) as described by Gauss's law[16]

$$\frac{\partial E}{\partial x} = \frac{q N_D}{\varepsilon_s}, \tag{1}$$

where x is the distance, q is the elementary charge, and N_D is the constant donor (Nb) concentration.

a)Electronic mail: a.m.kamerbeek@rug.nl

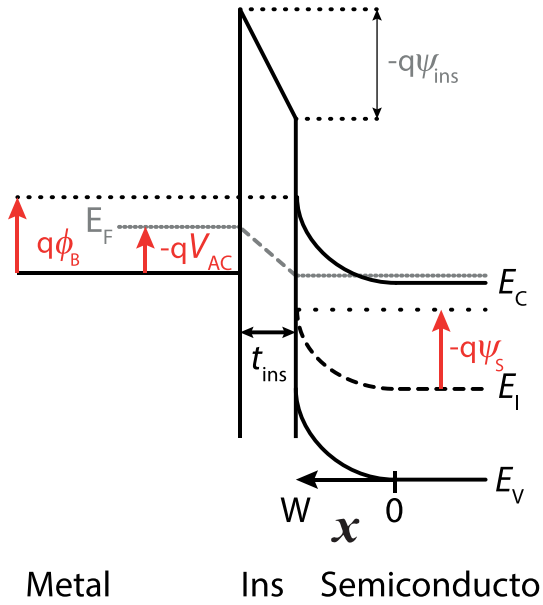

FIG. 1. Schematic band diagram for a M(I)S contact at an applied bias. The difference in the metal workfunction ϕ_m and the electron affinity χ in the semiconductor (e.g., $SrTiO_3$) gives rise to a potential barrier of height ϕ_B as well as a potential drop ψ_{ins} over the insulator. The ultra-thin (sub-nm) insulator thickness contributes to a dramatic lowering of ϕ_B yielding field emission.

The dielectric permittivity of $SrTiO_3$ is expressed as[10,11]

$$\varepsilon_s(T,E) = \frac{b(T)\,\varepsilon_0}{\sqrt{a(T)+E^2}}, \tag{2}$$

with T being the temperature and $\varepsilon_0 = 8.85\times10^{-14}$ F/cm and fit parameters $b(T) = 1.37\times10^7 + 4.29\times10^7\ \left(\frac{T}{100}\right)$ V/cm and $a(T) = [b(T)/\varepsilon_s(T,0)]^2$ V^2/cm^2, with

$$\varepsilon_s(T,0) = \frac{1635\,\varepsilon_0}{\coth\left(\frac{44.1}{T}\right) - 0.937}, \tag{3}$$

following Barrett's formula.[17]

After solving Eq. (1) using the boundary condition $E(0) = 0$, we obtain[11]

$$E(T,x) = \sqrt{a(T)}\,\sinh\left(\frac{qN_D x}{b(T)\,\varepsilon_0}\right). \tag{4}$$

From Eq. (4), we can write the potential as $\psi(x) = -\int E(x)dx$. Hence, with the boundary conditions $\psi(0) = 0$ and $\psi(W) = \psi_s$, we obtain

$$\psi(T,x) = \frac{b(T)\,\varepsilon_0}{qN_D}\sqrt{a(T)}\left[1-\cosh\left(\frac{qN_D x}{b(T)\,\varepsilon_0}\right)\right]. \tag{5}$$

From Eq. (5), we can derive a relation for the depletion width

$$W(T,\psi_s) = \frac{b(T)\,\varepsilon_0}{qN_D}\,\text{arccosh}\left(1-\psi_s\frac{qN_D}{b(T)\,\varepsilon_0\sqrt{a(T)}}\right), \tag{6}$$

with $\psi_s = \psi(T, x = W)$ being the surface potential. In the case of a MS system, ψ_s is independent of T.

The applied voltage can be expressed as

$$V_{AC} = \psi_s + V_{FB} = \psi_s + \frac{\phi_m - \phi_s}{q}, \tag{7}$$

with V_{FB} being the flat band voltage formed by the difference in the workfunction of the metal ($\phi_m = 5$ eV) and semiconductor ($\phi_s = 4.1$ eV), respectively. Also,

$$\phi_B = -\psi_s - \frac{E_F - E_c}{q} = -V_{AC} + V_{FB} - \frac{E_F - E_c}{q}, \tag{8}$$

with E_F being the Fermi level and E_c being the conduction band edge in the neutral semiconductor region. Therefore, the surface potential is a direct measure of ϕ_B, see Fig. 1.

The electrostatics in a MIS system is given by[16]

$$Q_{dep}(T,\psi_s) = -C_{ins}\,(V_{AC} - \psi_s - V_{FB}), \tag{9}$$

hence, the depletion charge depends on the voltage drop across the insulator layer times its areal capacitance $C_{ins} = \varepsilon_{ins}/t_{ins}$, where ε_{ins} and t_{ins} are the permittivity and thickness of the insulator, respectively. The depletion charge is defined by $Q_{dep} = qN_D\,W(T) = \int_0^{Emax}\varepsilon_s(T,E)\,dE$. This gives the following relation between applied bias and surface potential:

$$V_{AC} = \psi_s + V_{FB} - \frac{b(T)\,\varepsilon_0}{C_{ins}}\,\text{arccosh}\left(1-\frac{qN_D}{\sqrt{a(T)}b(T)\,\varepsilon_0}\,\psi_s\right). \tag{10}$$

Although Eq. (10) cannot be solved in a closed form to determine ψ_s, it is possible to plot it versus V_{AC}. In Fig. 2, the change of ψ_s (V_{AC}) is plotted while varying t_{ins}, N_D, and T separately. The values are $t_{ins} = 7$ Å, $T = 300$ K, $N_D = 2\times10^{19}$ cm^{-3}, and $V_{FB} = 0.9$ V when they are kept constant. In Fig. 2(a), t_{ins} is varied and shows a strong reduction of ψ_s

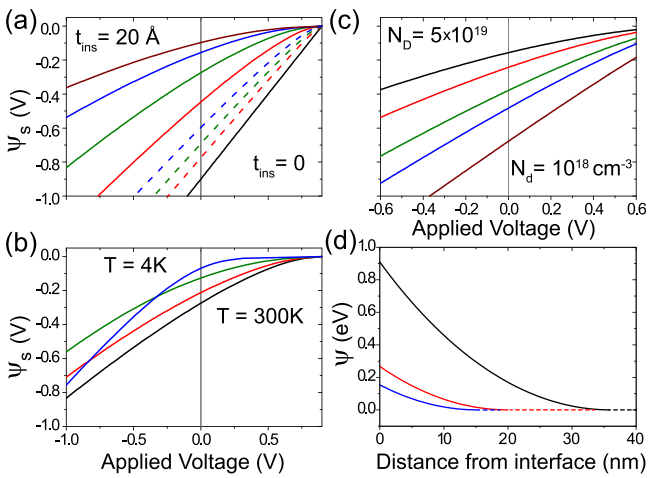

FIG. 2. The dependence of the surface potential ψ_s against the applied bias V_{AC} using Eq. (10) for the $SrTiO_3$-based MIS system as function of (a) insulator thickness (0, 4, 7, 11, and 20 Å), the dashed lines represent the change for n-Si MIS with all parameters the same except $\varepsilon_s = 11.9\,\varepsilon_0$, (b) temperature (300, 200, 100 to 4 K), and (c) doping density ($N_D = 10^{18}$, 5×10^{18}, 10^{19}, 2.5×10^{19} to 5×10^{19} cm^{-3}). In (d), the conduction band potential energy is shown for $t_{ins} = 0$, 7, and 11 Å for the black, red, and blue lines, respectively.

with increasing t_{ins}. For comparison, the change for an Si MIS ($\varepsilon_s = 11.9$) is also shown (dashed lines). A much larger reduction of the SBH (>0.7 V) is observed at zero bias compared with the Si MIS (~0.3 V). Since the t_{ins} values are relatively small, a much higher field emission (FE) current can be realized than in the case of an Si MIS system. The large reduction in the slope of ψ_s shows that the inclusion of a very thin insulator strongly reduces the gate action, as most of the applied voltage is absorbed by the low permittivity insulator. Hence, relatively large voltages are needed to modulate the n-$SrTiO_3$ conduction bands when a low permittivity (compared with ε_{STO}) gate insulator is used. Note that the observed trend for the $SrTiO_3$ MIS would be very similar to any semiconductor having a constant permittivity of $\varepsilon_s \approx 277$ (not shown). Hence, at T = 300 K, the built-in electric field is not high enough to cause significant non-linearity of ε_s.

When decreasing the temperature, the non-linear nature does have a strong effect, as shown in Fig. 2(b). A reduction of ψ_s at zero bias is observed indicating that the SBH is temperature dependent. Second, the slope is strongly determined by the temperature especially below ~50 K. In this temperature regime, the built-in field in the $SrTiO_3$ has a pronounced effect on the ε_s. This results in a sharper response of ψ_s at a negative V_{AC}, which increases the built-in electric field and hence reduces ε_s, causing a larger voltage drop in the semiconductor. The opposite happens for a positive bias resulting in a slow change. Note that this does not occur in a linear dielectric MIS (irrespective the value of ε_s). In Fig. 2(c), N_D is varied and shows that ψ_s is very sensitive to the doping density. At zero bias, a reduction larger than 0.7 V is realized at $5 \times 10^{19}\,cm^{-3}$, while for Si it is around 0.3 V (not shown).

In Fig. 2(d), the potential energy of the semiconductor surface region is given for $t_{ins} = 0$, 7, and 11 Å at 300 K and $N_D = 2 \times 10^{19}\,cm^{-3}$. A significant reduction of both the SBH ($V_{AC} = 0$ V) and depletion width are observed. Since the reduction of current flow due to the thin AlO_x tunnel barrier is low, a significant increase in the forward and reverse current is expected. Also note that the reduction of the barrier width and height suggests a strong increase of direct tunneling current compared with the Thermionic FE (TFE) for the Schottky device. Note that in the case of an interfacial layer, the flat band voltage (V_{FB}) could be affected by extrinsic charge, for which the most important ones are fixed (oxide) charge (Q_F) and interface trapped charge (Q_{it}) that depends on ψ_s (Ref. 14): $V_{FB} = (\phi_m - \phi_s)/q - Q_F/C_{ins} - C_{it} * \psi_s/C_{ins}$. Hence, a positive Q_F yields a drop in the SBH independent of the bias, while Q_{it} will induce a change in the SBH depending on the bias and the type of traps. In the case of acceptor-like traps, it will reduce the slope of the curves in Figs. 2(a)–2(c) and the SBH.

III. EXPERIMENT

To confirm the barrier lowering with increasing insulator thickness, we fabricated Co(20 nm)/AlO_x(*t*Å)/n-$SrTiO_3$ diodes with insulator thicknesses *t* of 0, 7, and 11 Å. We use the *I-V* measurements which were discussed qualitatively in Ref. 18 to extract quantitative values for the barrier lowering. The high quality of the diodes is expressed by the low value of the ideality factor $n \approx 1.3$ at room temperature for the Co/n-$SrTiO_3$ Schottky diode.[6]

For the Co/n-$SrTiO_3$ diode, we use the following relation to extract the Schottky barrier height at zero bias ϕ_{B0}

$$\phi_{B0} = \frac{\phi_{BF}}{n} + \left(\frac{n-1}{n}\right)\xi, \tag{11}$$

where ϕ_{B0} and the ideality factor *n*, obtained from thermionic-emission fits of the temperature dependent *I-V*'s,[18] are related to a more fundamental barrier height ϕ_{BF} at flat band condition and the electron degeneracy of the semiconductor ξ.[19] In Fig. 3(a), we plot 1/n versus ϕ_{B0} and fit the data with Eq. (11). We find $\phi_{BF} = 0.9 \pm 0.03$ V and $\xi = -32 \pm 0.01$ meV, which agree very well with the expected flat band voltage of 0.9 V and semiconductor degeneracy between −20 and −50 meV, where ξ is estimated using a parabolic band approximation. Note that a negative value of ξ indicates a degenerate semiconductor. A conventional fit of the *I-V* at room temperature using the thermionic-emission model results in ϕ_{B0} of 0.63 V indicating a large underestimation of ϕ_B.

In the MIS diodes, a much larger contribution arises from electron tunneling through the barrier. To estimate the SBHs, a Richardson plot is made as shown in Fig. 3(b), using a Richardson constant A^* of 156 $cm^{-2}\,K^{-2}$ and an effective mass $m^* = 1.3\ m_0$.[20] The saturation current I_S is extracted from the temperature dependent *I-V*'s using $I = I_S \exp(qV_{AC}/nkT)$. The plot is fitted using the expressions for I_S in the TFE ($t_{ins} = 7$ Å) and FE regime ($t_{ins} = 11$ Å) (solid black lines).[21] To account for the reduction in *I* due to the tunnel barrier, we multiply the expressions for I_S with $\exp(-\alpha d \phi_T^{1/2})$ where $\alpha = 2(2m^*)^{1/2}/\hbar$, *d* is the barrier width (in Å), and ϕ_T is the (effective) barrier height and set to 1.5 V. We obtain the values for the fit parameters E_{00}, ϕ_B, and ξ which relate to the transport via tunneling versus thermal emission, the effective SBH, and the semiconductor degeneracy, respectively. The barrier height extracted using this method is the electrical equivalent of the MS junction; hence, it could deviate at least

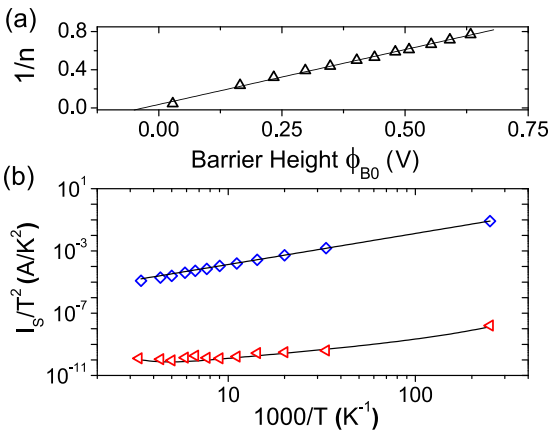

FIG. 3. (a) Plot of 1/n against ϕ_{B0} (black triangles) fitted with Eq. (11) (black line). A flat band barrier height ϕ_{BF} of 0.9 ± 0.03 V is obtained. (b) Richardson plot extracted from the temperature dependent *I-V* measurements for the diodes with $t_{ins} = 7$ Å (red triangles) and 11 Å (blue diamonds). A good fit is obtained using the TFE model for the first, while the latter can only be fitted by a FE model (black lines). The obtained Schottky barrier heights ϕ_B are 0.45 ± 0.1 and 0.15 ± 0.1 V, respectively.

partly from the actual SBH inside the semiconductor and is referred to as the effective SBH. The relative change of the effective barrier is well reflected by such an analysis.[22,23]

Transport occurs via TFE when $kT \approx E_{00}$ and FE when $E_{00} \gg kT$. The change from thermally assisted to direct tunneling transport is well expressed by the large increase of E_{00} from 37 meV to 350 meV. For ξ, we find -36 and -60 meV, which are close to the estimated values. For ϕ_B, we find 0.45 ± 0.1 V and 0.15 ± 0.1 V. Although a Richardson plot for the Co/n-$SrTiO_3$ diode was made, a good fit with either the TFE or FE expression could not be obtained. In the first instance, this might be surprising but the large reduction in the semiconductor ψ_s for the MIS diodes reduces the influence of the non-linear ε_s on the charge transport leading to better fits for the MIS diodes. Note that the expressions for I_S do not include the change in barrier shape due to the non-linear ε_s. Therefore, the extracted values serve to establish the relative trend in decreasing surface potential, hence ϕ_B, rather than to give an absolute comparison with the electrostatic calculations.

In Fig. 4, we plot the obtained values for the SBH at $V_{AC} = 0$ V with increasing t_{ins} for the n-$SrTiO_3$ MIS diodes at room temperature as obtained from the electrostatic model (blue diamonds). The model shows relatively good agreement with the extracted values of the SBHs (red circles). For comparison, the trend for an n-Si MIS diode is shown as well. Although studies show that a sizable reduction of the contact resistance can be achieved for n-Si MIS systems, this is attributed to the reduction of interface induced gap states.[24] For the $SrTiO_3$ MIS system, the model indicates that the reduction can be fully attributed to the relative permittivity of $SrTiO_3$. Unlike conventional semiconductors, it is thus possible to realize a large reduction in the SBH for metals with large workfunctions even when Fermi level pinning is absent.

Finally, we discuss the relative effects of barrier lowering expected from the image force relative to the electrostatic screening in the metal. First, the image force effect causes a barrier lowering $\Delta\phi \propto (N_D/\varepsilon_s^3)^{1/4}$; hence, this effect is small for large ε_s. The barrier lowering due to electrostatic screening originates from a lowering of the metal workfunction due to the finite screening length of the charge sheet $Q_m = Q_{dep} = qN_D W(T)$ at the metal interface. In this case, $\Delta\phi \propto (N_D\,\varepsilon_s)^{1/2}$ and is thus expected to be relatively large for the n-$SrTiO_3$ diodes.[25,26] Note that the charge density in the metal Q_m is much larger compared with that in conventional semiconductor M(I)S systems.

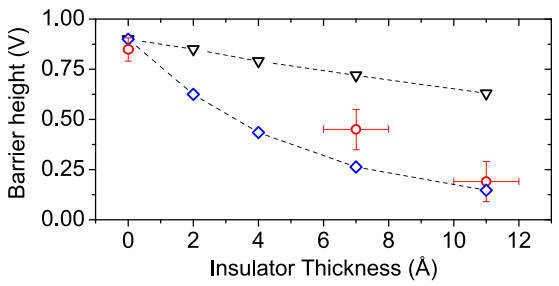

FIG. 4. The experimental Schottky barrier height against the AlO_x layer thickness t_{ins} (red circles). The model for the $SrTiO_3$-based M-I-S system (blue diamonds line) shows relatively good agreement. For comparison, the results obtained for the modeled Si counterpart (black triangles) are also shown. Material parameters used are $\phi_m = 5$ eV, $\phi_s = 4.1$ eV, $N_D = 3 \times 10^{19}$ cm^{-3}, $\varepsilon_{ins} = 9.6$, and $T = 300$ K.

As can be inferred from Fig. 2, both ψ_s and ε_s are strongly modulated by varying t_{ins} and V_{AC}. Therefore, both the insertion of a thin insulator and biasing the junction allow a large manipulation of Q_m. This could be useful for realizing surface magneto-electric effects when the metal is a ferromagnet which is of particular interest for realizing spintronic devices.[27]

IV. CONCLUSIONS

In this work, we show that despite its degeneracy rectification is possible in the $SrTiO_3$-based Schottky contact confirming the experimental data. In addition, in the MIS system, the SBH is strongly reduced by the insulator layer compared with that of silicon. We show that this leads to a higher current (via tunneling) compared with a pure Schottky contact as confirmed by experiments. The dependence of the surface potential and depletion width is shown to exhibit strong temperature and doping density dependence unlike conventional semiconductors with constant permittivity. The understanding of these influences on the electrostatic potential is important for designing M/I/n(p)-$SrTiO_3$ interfaces/devices. Finally, we would like to note that to obtain a complete *I-V* model, the incorporation of a tunneling model and high injection effects is required.

ACKNOWLEDGMENTS

A.M.K. and T.B. acknowledge the financial support from the Netherlands Organization for Scientific Research NWO-VIDI program and the Rosalind Franklin Fellowship.

[1]D. Connely, C. Faulkner, D. E. Grupp, and J. S. Harris, IEEE Trans. Nanotechnol. **3**, 98 (2004).
[2]E. I. Rashba, Phys. Rev. B **62**, R16267(R) (2000).
[3]A. Fert and H. Jaffrés, Phys. Rev. B **64**, 184420 (2001).
[4]C. Capan, G. Y. Sun, M. E. Bowden, and S. A. Chambers, Appl. Phys. Lett. **100**, 052106 (2012).
[5]M. Stengel and N. Spaldin, Nature **443**, 679 (2006).
[6]E. Mikheev, B. D. Hoskins, D. B. Strukov, and S. Stemmer, Nat. Commun. **5**, 3990 (2014).
[7]A. Verma, S. Raghavan, S. Stemmer, and D. Jena, Appl. Phys. Lett. **105**, 113512 (2014).
[8]A. Ohtomo and H. Y. Hwang, Nature **427**, 423 (2004).
[9]Y. Z. Chen, N. Bovet, F. Trier, D. V. Christensen, F. M. Qu, N. H. Andersen, T. Kasama, W. Zhang, R. Giraud, J. Dufouleur, T. S. Jespersen, J. R. Sun, A. Smith, J. Nygård, L. Lu, B. Büchner, B. G. Shen, S. Linderoth, and N. Pryds, Nat. Commun. **4**, 1371 (2013).
[10]S. Suzuki, T. Yamamoto, H. Suzuki, K. Kawaguchi, K. Takahashi, and Y. Yoshisato, J. Appl. Phys. **81**, 6830 (1997).
[11]T. Yamamoto, S. Suzuki, K. Kawaguchi, and K. Takahashi, Jpn. J. Appl. Phys., Part 1 **37**, 4737 (1998).
[12]H. Takauchi, A. Yoshida, H. Tamura, T. Imamura, and S. Hasuo, Appl. Phys. Lett. **61**, 1462 (1992).
[13]T. Yajima, M. Minohara, C. Bell, H. Kumigashira, M. Oshima, H. Y. Hwang, and Y. Hikita, Nano Lett. **15**, 1622 (2015).
[14]D. K. Schroder, *Semiconductor Material and Device Characterization*, 3rd ed. (John Wiley & Sons, Inc., USA, 2006).
[15]E. H. Rhoderick and R. H. Williams, *Metal-Semiconductor Contacts*, 2nd ed. (Clarendon, Oxford, 1988).

[16]S. M. Sze and K. K. Ng, *Physics of Semiconductor Devices*, 3rd ed. (John Wiley & Sons, Inc., USA, 2007).
[17]J. H. Barrett, Phys. Rev. **86**, 118 (1952).
[18]A. M. Kamerbeek, E. K. de Vries, A. Dankert, S. P. Dash, B. J. van Wees, and T. Banerjee, Appl. Phys. Lett. **104**, 212106 (2014).
[19]L. F. Wagner, R. W. Young, and A. Sugerman, IEEE Electron Device Lett. **4**, 320 (1983).
[20]Z. Sroubek, Phys. Rev. B **2**, 3170 (1970).
[21]F. A. Padovani and R. Stratton, Solid-State Electron. **9**, 695 (1966).
[22]Y. Zhou, M. Ogawa, X. Han, and K. L. Wang, Appl. Phys. Lett. **93**, 202105 (2008).
[23]D. Lee, S. Raghunathan, R. J. Wilson, D. E. Nikonov, K. Saraswat, and X. S. Wang, Appl. Phys. Lett. **96**, 052514 (2010).
[24]W. Monch, J. Appl. Phys. **111**, 073706 (2012).
[25]S. S. Perlman, IEEE Trans. Electron Devices **16**, 450 (1969).
[26]Y. Hikita, M. Kawamura, C. Bell, and H. Y. Hwang, Appl. Phys. Lett. **98**, 192103 (2011).
[27]C. Duan, J. P. Velev, R. F. Sabirianov, Z. Zhu, J. Chu, S. S. Jaswal, and E. Y. Tsymbal, Phys. Rev. Lett. **101**, 137201 (2008).